Synthetic Metals, 2 (1980) 99 - 107

OPTICAL STUDIES OF THE HIGH-FREQUENCY GRAPHITIC INTRALAYER PHONONS IN GRAPHITE–$SbCl_5$

P. C. EKLUND, D. S. SMITH and V. R. K. MURTHY

Department of Physics and Astronomy, University of Kentucky, Lexington, KY 40506 (U.S.A.)

S. Y. LEUNG

Center for Materials Science and Engineering, Massachusetts Institute of Technology, Cambridge, MA 02139 (U.S.A.)

(Received June 16, 1980)

Summary

We report on the Raman and infrared spectra for well characterized samples of stages 2 - 5 $SbCl_5$–graphite. The first order Raman and infrared spectra show stage dependent behavior similar to that observed in other graphite intercalation compounds. The first order spectral features in the Raman and infrared spectra are interpreted in terms of Γ-point bounding and interior layer vibrational modes of the carbon atoms. These Γ-point modes stiffen with increasing reciprocal stage number ($1/n$). We also report the first systematic study of the stage dependence of the second order Raman spectrum of a graphite intercalation compound. We find well defined second order spectral features closely related to those found in HOPG. We interpret the above findings in terms of an extended (graphitic) zone scheme.

1. Introduction

In the past several years experimental studies of Raman-active phonons in graphite intercalation compounds have been reported for both donor- and acceptor-type systems [1]. More recently, through the application of Fourier transform spectroscopy, information concerning infrared active modes has become available [2, 3, 4]. To a large extent the previously reported experimental work on optically-active phonons in graphite intercalation compounds has concentrated on the stage dependent behavior of graphitic, intra-layer phonons associated with the central (Γ) point in the hexagonal Brillouin zone of the host graphite material.

In this paper we present results of the first reported observations of intercalation-induced changes in graphitic intralayer phonons associated with

points other than the central (Γ) point in the graphite Brillouin zone. These newly reported modes are associated with the zone-interior (Σ, T) and zone-edge (T′) points in the graphite zone. High frequency phonons associated with these points can be studied in the second order (2-phonon) Raman spectra of graphite intercalation compounds. They manifest themselves in the overtone region of the Raman spectrum as reasonably sharp features which allow semi-quantitative information to be easily extracted from the data without having to resort to a two-phonon density of states calculation.

The stage dependence of these modes, along with that of the Γ-pt derived Raman- and infrared-active modes is reported for the stage 2, 3, 4, 5 compounds of $SbCl_5$–graphite. The phonon data presented in this work represents the most complete set of stage-dependent information currently available on the high-frequency graphitic intra-layer phonons in a graphite intercalation compound.

2. Experimental

The stage 2 - 5 samples of $SbCl_5$–graphite were prepared by reacting highly oriented pyrolytic graphite (HOPG) with the vapors of doubly distilled $SbCl_5$. The procedures used by us to prepare these compounds have been discussed elsewhere [5].

The samples were characterized using: (1) X-ray diffraction; (2) Raman scattering; (3) visible and near infrared spectroscopy (0.2 - 3.0 eV); (4) Fourier transform spectroscopy (0.05 - 0.5 eV). Data taken on saturated (stage 2) compounds handled in room air were found to be identical with data taken on samples kept in an overpressure of $SbCl_5$ since the commencement of the intercalation reaction. Furthermore, these measurements were repeated on the air-exposed samples several times over a three-month period and yielded repeatable results. That is, the optical spectra and the position and FWHM of the (00l) peaks in the X-ray scans remained unchanged [5]. In the time between these measurements the samples were stored in dry air over desiccant ($CaSO_4$). These results lead us to conclude that $SbCl_5$–graphite samples are reasonably stable in laboratory air and are particularly well suited for characterization by a broad range of techniques. We should point out, however, that our experiments may not be particularly sensitive to the concentration of neutral intercalated species. It is therefore possible that these neutral molecules are not stable residents under ambient conditions. Experiments are underway which will address this issue. At this time we can say that our optical data strongly suggest that the lattice dynamical and electronic properties of $SbCl_5$–graphite are not affected by exposure of the samples to laboratory air.

The optical techniques used in collecting the Raman and Fourier Transform spectra presented in this work have been discussed in detail elsewhere [2, 6].

3. Discussion of results

In Fig. 1(a) we show the recently calculated phonon dispersion curves [7] of pristine graphite by Maeda *et al.* The hexagonal Brillouin zone of pristine graphite is shown in Fig. 1(b). A symmetry analysis of the zone center phonons of pristine graphite shows that there are two high-frequency Raman-active (E_{2g}) modes and three high-frequency infrared-active (E_{1u}, A_{2u}) modes. The A_{2u} mode (867 cm^{-1}) [8] involves out-of-plane (*c*-axis) carbon atom motion and can only be observed on the *a*-face. The E_{1u} (1587 cm^{-1}) and E_{2g} (1582 cm^{-1}) modes are intralayer modes and can be studied with radiation incident on the *c*-face. Second-order Raman scattering with radiation incident on the *c*-face, can also be used to study other graphitic intralayer modes with large crystal momentum. The second-order Raman spectra of crystals are often complex, exhibiting overlapping contributions from combination ($\omega_1 \pm \omega_2$) and overtone (2ω) 2-phonon scattering. However, the second-order Raman spectra of graphite and $SbCl_5$–graphite are relatively simple, being dominated by sharp features associated with overtone (2ω) scattering. The spectral positions of these sharp features can then be simply related to the phonon frequency of the approximately degenerate pair of scattered phonons.

Furthermore, because of the similarity of the second-order Raman spectra of $SbCl_5$–graphite to that of the parent graphite material itself, the features in the spectra of the intercalation compounds can be understood in terms of modified graphitic intralayer phonons with phonon-frequency shifts induced by the various stages of $SbCl_5$ intercalation. Before proceeding to the analysis of the second order spectra of the $SbCl_5$–graphite intercalation compounds, we first discuss the results obtained for the Raman- and ir-active Γ-pt derived modes in these materials which make contact with previously published work in other acceptor compounds.

In Fig. 2 we show the Raman spectra of stage 2 - 5 $SbCl_5$–graphite and HOPG in the 1600 cm^{-1} region of the E_{2g} graphite intralayer mode. In agreement with earlier work [1 - 4, 6, 9] on both donors and acceptor com-

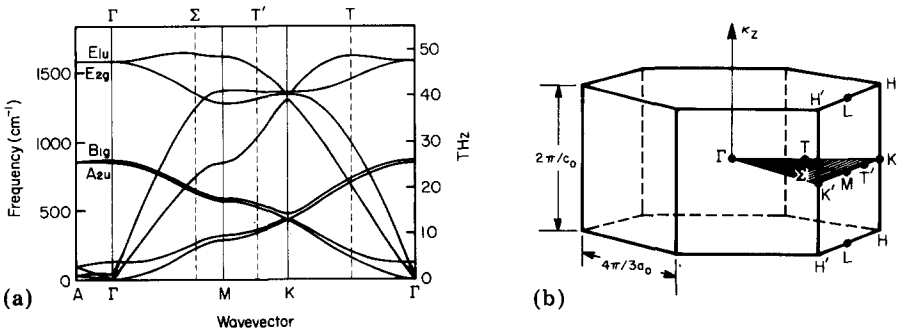

Fig. 1. (a) Phonon dispersion curves of graphite (ref. 7). (b) Hexagonal Brillouin zone of graphite.

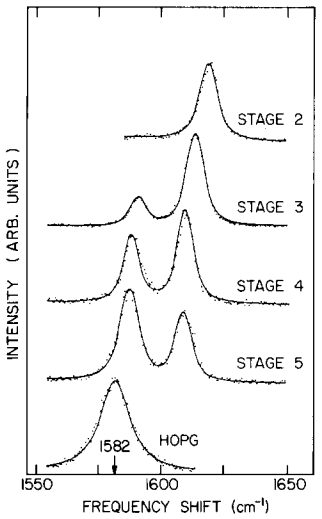

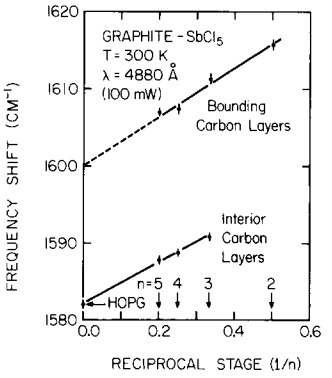

Fig. 2. Raman spectra of the zone center phonons of HOPG and stage 2 - 5 $SbCl_5$–graphite. The solid lines represent the results of a Lorentzian lineshape analysis.

Fig. 3. A graph of the zone-center Raman-active phonon frequencies plotted *vs.* reciprocal stage $(1/n)$. The straight lines were determined by a least squares fit to the data.

pounds, a Raman doublet is observed for stages $n > 2$, and a single line is observed for the stage 2 compound. Previous works have identified the lower and higher frequency components of the doublet with graphitic intralayer (Γ-pt) modes in interior and bounding carbon layers, respectively. Stage 2 compounds exhibit a single Raman line in this region of the spectrum because they contain only bounding carbon layers. Figure 3 shows a graph of the Raman-active bounding and interior carbon layer mode frequencies plotted *vs.* reciprocal stage $(1/n)$. A linear relation is apparent in the Figure, with the modes stiffening with increasing reciprocal stage. These results are consistent with all the previously published Raman scattering work on Γ-pt derived modes in other acceptor compounds.

The ir-active phonons were studied using Fourier Transform Spectroscopy. The absolute reflectance $R(\omega)$ of the samples was measured at near normal incidence in dry nitrogen. R is related to the optical constants n and k by the well known relation

$$R(\omega) = \frac{(n-1)^2 + k^2}{(n+1)^2 + k^2} \tag{1}$$

where the complex refractive index $n_* = n + ik$ is related to the complex dielectric constant $\epsilon_* = \epsilon_1 + i\epsilon_2$ *via* $\epsilon_* = n_*^2$. The complex dielectric constant can be represented by the sum of three contributions,

$$\epsilon_*(\omega) = \epsilon_\infty + \epsilon_{\text{electronic}} + \epsilon_{\text{phonon}} \tag{2}$$

where ϵ_∞ is the contribution from the core (high energy processes) and $\epsilon_{\text{electronic}}$ represents the contribution from intraband and low energy inter-

band electronic transitions. Details concerning $\epsilon_{electronic}$ can be found in another article in this volume by Eklund *et al.* [10]. The contribution ϵ_{phonon} to the complex dielectric constant from the infrared-active phonons is represented as a collection of oscillators,

$$\epsilon_{phonon} = \sum_{\alpha} \frac{f_\alpha {\omega_\alpha}^2}{(\omega_\alpha - \omega)^2 + i\Gamma_\alpha \omega} \tag{3}$$

where f_α, ω_α and Γ_α are, respectively, the oscillator strength, the frequency and the damping parameters for oscillator, α. It should be noted that the values of these phonon parameters are not particularly sensitive to the details [10] of electronic contribution. The scans of the infrared-active phonons of stage 2 - 5 $SbCl_5$–graphite in the 1600 cm^{-1} region of the graphitic (E_{1u}) intralayer mode are shown in Fig. 4. As can be seen in the Figure the phonon structure shifts to higher frequency with decreasing stage number, which is consistent with the behavior of the Raman-active Γpt derived phonons (Fig. 2). Although they are not well resolved in the data, there are three phonons apparent in the stage $n > 2$ data, and 2 phonons contribute to the reflectance structure of the stage 2 compound. The phonon (or oscillator) parameters are determined by the lineshape analysis defined by eqns. (1) - (3). In Fig. 5 we show the phonon frequencies, ω_α, plotted *vs.*reciprocal stage ($1/n$). The lines in the Figure are guides to the eye. The highest frequency modes for stages 3, 4, 5 can be seen to fall on a line which extrapolates back to the value reported for the E_{1u} mode in HOPG. We therefore associate these

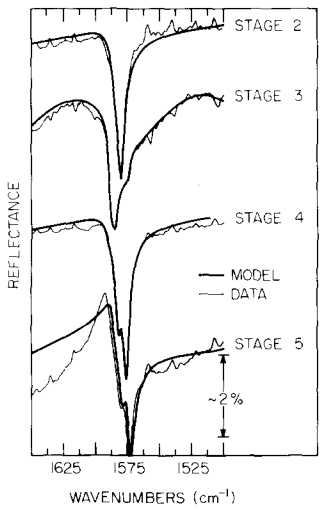

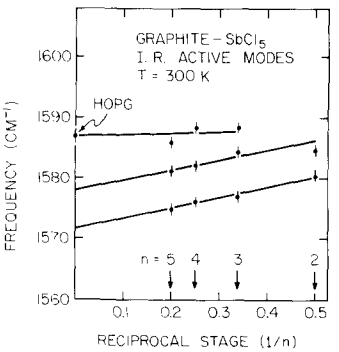

Fig. 4. Reflectance spectra of the infrared-active phonons of stage 2 - 5 $SbCl_5$–graphite. The stage 3 data have a superimposed sinusoidal background which is instrument-related. This background was included in the stage 3 lineshape analysis.

Fig. 5. Graph of the infrared phonon frequencies plotted as a function of reciprocal stage for $SbCl_5$–graphite. The straight lines are guides for the eye.

modes with the interior carbon layers. This interpretation is also consistent with a third, higher-frequency ir mode being absent in the stage 2 compound (which does not contain interior layers). The two lowest frequency modes for each stage compound can then be tentatively assigned to Γ-pt derived graphitic intralayer modes associated with the bounding layers. The full list of oscillator lineshape parameters used to fit the phonon features in the infrared reflectance spectra of stage 2 - 5 $SbCl_5$–graphite is given in Table 1.

TABLE 1

Oscillator parameters (eqn. (3)) used to fit the infrared-active phonon features in the reflectance spectra of stage 2 - 5 $SbCl_5$–graphite shown in Fig. 4.

Stage	ω_α (cm^{-1})	$2\Gamma_\alpha$ (FWHM) (cm^{-1})	f_α
2	1580.4	6	0.16
	1585	10	0.12
3	1577	8	0.03
	1584.5	8	0.065
	1588.5	6	0.088
4	1576.3	5	0.08
	1582.3	7	0.14
	1588.5	8	0.035
5	1574.8	5	0.035
	1581.3	8	0.062
	1586	5	0.02

We now turn our attention to the results of the second order Raman scattering studies in these compounds. First, we review the second-order Raman spectrum of pristine graphite which is shown in Fig. 6. In addition to the strong first-order peak seen at 1582 cm^{-1}, several features at higher frequencies are apparent in the frequency range $1600 < \omega < 3400$ cm^{-1}. These features were analyzed in a recent paper by Nemanich and Solin [11]. The data shown in Fig. 6 are in good agreement with their work; structure is seen at 2429 cm^{-1} (T′), 2697 cm^{-1} (T′), 2737 (T′) and 3248 cm^{-1} (Σ, T). The letters in parentheses label the respective points in the graphite Brillouin zone (Fig. 1). As can be seen in Fig. 1(a), the positions T′, T and Σ in the high frequency optical branches locate regions of low dispersion and are thus also associated with high 2-phonon density of states and strong second-order overtone Raman scattering. Because the second order Raman spectra of stage 2 - 5 $SbCl_5$–graphite closely resemble that observed in pristine graphite, we can interpret the spectra of the intercalation compounds using an extended (graphitic) zone scheme. The actual Brillouin zone of the intercalation compound is, of course, much smaller due to c-axis zone-folding interactions

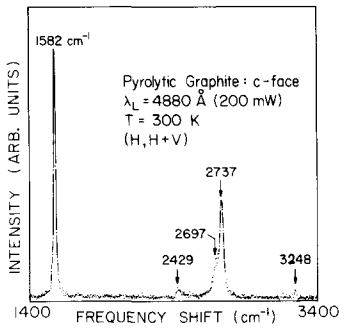

Fig. 6. High-frequency Raman spectra of HOPG. The features for $\omega > 1600$ cm^{-1} are associated with overtone scattering from zone-interior and zone-edge phonons.

associated with staging. As the intercalate layer is probably not very well-ordered, in-plane zone-folding effects are expected to be much less important.

Turning our attention to the second order Raman spectra of $SbCl_5$–graphite, we see in Fig. 7 that the spectra of the stage 2 - 5 compounds are, indeed, similar in form to that of pristine graphite. The spectra of HOPG is shown at the bottom of the panels. Panel A covers the region from 2350 to 2900 cm^{-1} and panel B the region 3200 - 3280 cm^{-1}. Beginning with the lowest energy features located at ~2429 cm^{-1} in panel A, we see that decreasing the stage number from $n = \infty$ (HOPG) to $n = 2$ transforms the

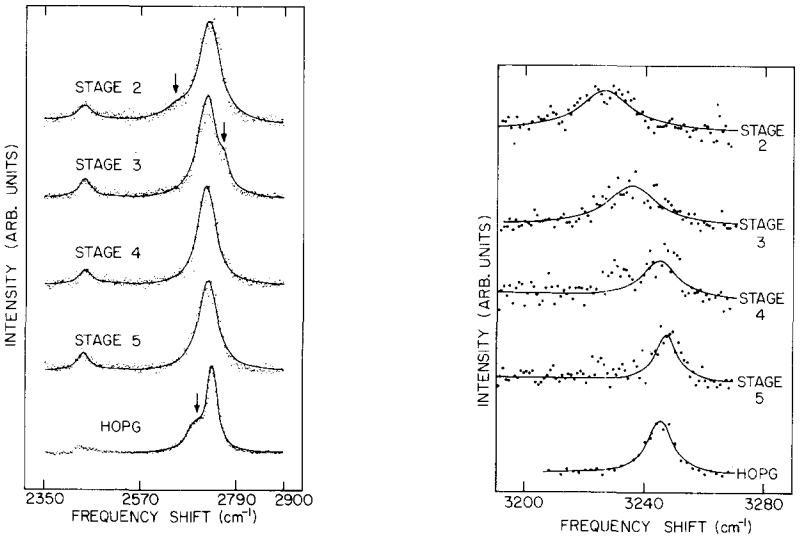

(A) (B)

Fig. 7. (Panel A) Second-order Raman spectra of stage 2 - 5 $SbCl_5$–graphite and HOPG in the region 2350 - 2900 cm^{-1}. The solid lines are the result of a Lorentzian lineshape analysis. (Panel B) Second-order Raman spectra of stage 2 - 5 $SbCl_5$–graphite and HOPG in the 3200 - 3280 cm^{-1} region. The solid lines represent a least squares fit of a single Lorentzian line to the data. The intensity of the scattering is ~ 3% of the first order peak at 1582 cm^{-1}.

graphitic feature associated with the T'pt from an asymmetric to a symmetric lineshape, suggesting a small change in the local dispersion; the position is left essentially unchanged. The structure at ~2700 cm^{-1} associated with the higher energy T'pt-derived intralayer modes also undergoes a change of shape with the center frequency remaining essentially constant. The data in this panel indicate that the low dispersion in the high frequency optical branches along the zone edge between the M and K points is preserved and largely insensitive to staging. The higher frequency features shown in panel B show contrasting behavior. They exhibit a clear downshift in frequency with decreasing stage. These modes are derived from the (Σ, T) zone-interior intralayer modes. The scattered light from these phonons is quite weak and the resulting poorer signal to noise ratio prevents us from observing a potential splitting in the 3248 cm^{-1} graphitic feature in going from a stage ∞ - (HOPG) to a stage 2 compound; we, therefore, have analyzed the structure as a single line. The solid curves in panel B represent the results of a least squares fit of a Lorentzian lineshape to the data. The lineshape analysis indicates a concomittant broadening and downshifting of these (Σ, T) phonons.

Finally, Fig. 8 summarizes the stage dependence of all the high-frequency Raman-active phonons studied in this work. As we have discussed, these graphitic, intralayer phonons are modified by the presence of the intercalated acceptor molecules. Shown in the Figure are the various phonon frequencies plotted *vs.* Reciprocal stage ($1/n$). As can be seen in the Figure a variety of stage dependent behavior is present. The Γ-pt derived intralayer modes stiffen with increasing reciprocal stage, which is in contrast to the behavior of the zone-interior (Σ, T) modes which soften, and the zone-edge (T') modes which suffer little change upon intercalation. Of special interest is the "crossover" of the zone-center (Γ) and zone-interior (Σ, T) derived modes at

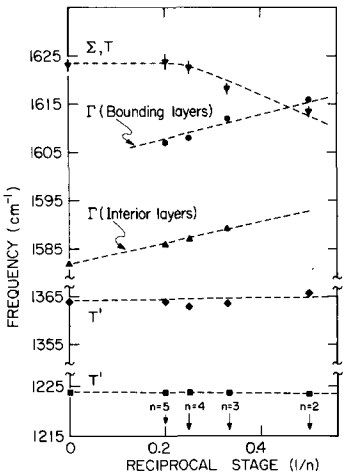

Fig. 8. Stage dependence of the high-frequency intralayer graphitic phonons studied in the first- and second-order Raman spectra of $SbCl_5$–graphite. The letters indicate the respective positions in the extended (graphitic) zone.

a stage 2 compound, indicating that the location of maximum phonon frequency is shifted by the intercalation process from the zone-interior derived modes to the Γ-pt derived modes.

4. Conclusion

We have presented the results of a spectroscopic study of the high-frequency, carbon atom intralayer modes in the acceptor compounds of stage 2 - 5 $SbCl_5$–graphite. The data have been interpreted in terms of an extended (graphitic) zone scheme. The results of this study represent the most complete set of stage-dependent, high frequency lattice mode data available for a single graphite intercalation system, having gathered information about both ir- and Raman-active phonons associated with many points in the extended Brillouin zone. We hope that these data will serve as an additional incentive for further theoretical studies of the lattice dynamics of graphite intercalation compounds.

Acknowledgements

We thank Professor C. Brock for the use of her X-ray equipment, and Professor K. Subbaswamy for helpful discussions.

The Fourier Transform Spectroscopy experiments were done at the Center for Materials Science (M.I.T.) in the laboratory of Professor M. S. Dresselhaus. We are very grateful for the encouragement and helpful comments of M. S. Dresselhaus and G. Dresselhaus during the course of this work. This work was supported in part by a grant from the Research Corporation. The Fourier Transform Spectroscopy was funded by the Office of Naval Research (ONR # N00014-77-C-0053).

References

1 M. S. Dresselhaus and G. Dresselhaus, in F. Lévy, (ed.), *Intercalated Layer Materials*, D. Reidel, Dordrecht, Holland, 1979, p. 423.
2 G. M. Gualberto, C. Underhill, S. Y. Leung and G. Dresselhaus, *Phys. Rev. B, 21* (1980) 862.
3 C. Underhill, S. Y. Leung, G. Dresselhaus and M. S. Dresselhaus, *Solid State Commun., 29* (1979) 769.
4 S. Y. Leung, C. Underhill, G. Dresselhaus and M. S. Dresselhaus, *Solid State Commun., 33* (1980) 285.
5 V. R. K. Murthy, D. S. Smith and P. C. Eklund, *Mater. Sci. Eng., 45* (1980) 77.
6 P. C. Eklund, E. R. Falardeau and J. E. Fischer, *Solid State Commun., 32* (1979) 631.
7 M. Maeda, Y. Kuramoto and C. Horie, *J. Phys. Soc. Jpn., 47* (1979) 337.
8 R. J. Nemanich, G. Lucovsky and S. A. Solin, *Solid State Commun., 23* (1977) 117.
9 P. C. Eklund, G. Dresselhaus, M. S. Dresselhaus and J. E. Fischer, *Phys. Rev. B, 21* (1980) 4705.
10 P. C. Eklund, D. S. Smith and V. R. K. Murthy, *Synth. Met., 3* (1981) in press.
11 R. J. Nemanich and S. A. Solin, *Phys. Rev. B, 20* (1979) 392.